

# A contribution to the mechanical characterization of polymeric coatings by depth-sensing indentation measurements

B. ROTHER

*Forschungsinstitut für Edelmetalle und Metallchemie, Katharinenstr. 17,  
D-73525 Schwäbisch Gmünd, Germany*

Coating–substrate systems consisting of polypropylene coatings with thicknesses of 6 and 9.8  $\mu\text{m}$  on silicon are investigated by depth-sensing indentation measurements with end loads between 20 and 1000 mN. Different effective load rates were applied. The results are correlated to an energy- and volume-related interpretation of the deformation processes. The proposed model permits to proof constant material behaviour over extended penetration depths. The potential on the quantification of the viscoelastic character as well as on the compound strength must be further verified.

## 1. Introduction

Polymeric coatings with thicknesses of up to some 10  $\mu\text{m}$  are increasingly used in several high-tec and engineering applications such as microelectronic packaging [1] and as protective coatings against stone and rain impact [2]. The measurement of mechanical characters of these coatings such as hardness, viscoelastic behaviour and compound strength is, however, not substantially solved yet. Hardness and modulus of the coatings are usually determined by indentation measurements including depth-sensing methods [3, 4]. The results of these measurements are generally considered critically because of tip rounding, surface artefacts and substrate effects [4]. Measurement parameters, such as indentation rate and mode, additionally effect the results.

Recently, an energy-related approach to the evaluation of depth-sensing indentation experiments has been reported [5]. This approach permits calculation of a hardness equivalent which remains constant over extended penetration ranges for homogeneous bulk materials such as metals, ceramics and polymers [6]. Based on the same approach, coating–substrate systems, consisting of hard coatings on metallic substrates, have also been investigated [7].

The present work was directed at the application of the energy-related evaluation of depth-sensing indentation measurements to the characterization of polypropylene coatings on silicon wafers. The investigations focused on medium penetration depth ranges where usually dominating effects of the substrate material are expected. For reasons of lucidity, a short summary of the energy-related approach will first be given.

## 2. Energy-related evaluation of depth-sensing indentation measurements

### 2.1. Homogeneous bulk materials

The approach starts from the existence of a limited and indenter-specific sample range (energy densification zone, EDZ) where the shift energy of the indenter,  $W_I$ , is transformed into deformation energy. For this sample range, mean densities of the deformation energy are defined which are related to the volume and the areas of the range. Additionally, characteristic extensions of the volume and the areas of the EDZ are defined to be linearly dependent on the penetration depth of the indenter. The energy balance thus reads

$$W_I = \bar{w}_V k_V s^3 + \bar{w}_A k_A s^2 = e_V s^3 + e_A s^2 \quad (1)$$

where  $\bar{w}_V$  and  $\bar{w}_A$  are the mean energy densities related to the volume and the areas, respectively,  $k_V$  and  $k_A$  are shape factors,  $s$  is the penetration depth of the indenter and  $e_V$  and  $e_A$  are indenter-specific energy densities. The EDZ is expected to expand under the action of the penetrating indenter against the resistance of the neighbouring material.

The relation of Equation 1 to the experimental magnitudes force and penetration depth, follows from the second derivative  $d^2W/ds^2$  which is identical to the first derivative of the force in relation to the penetration depth. Thus we obtain

$$\begin{aligned} \frac{d^2W_I}{ds^2} &= \frac{dF}{ds} \\ &= 6\bar{w}_V k_V s + 2\bar{w}_A k_A \\ &= 6e_V s + 2e_A \end{aligned} \quad (2)$$

Proof for Equation 1 thus follows from the appearance of linear ranges in the first derivative of the force in relation to the penetration depth,  $s$  (differential load feed, DLF) for at least limited penetration depths. An experimental confirmation of the approach was recently given for different classes of material probed with a Vickers indenter [6].

## 2.2. Coating materials

The expansion of the EDZ in coating materials has already been described in detail elsewhere [7]. Those reported results for hard coatings on metallic substrates could be well correlated to the following assumptions.

1. The expansion of the EDZ in the homogeneous coating material is comparable to that for homogeneous bulk materials until the outer face of the densification zone reaches the interface to the substrate material. For the energy balance we thus obtain

$$W_I = \bar{w}_{VC} k_{VC} s^3 + \bar{w}_{AC} k_{AC} s^2 \quad (3)$$

with the specific energy densities and shape factors of the coating material (index C).

2. After the outer face of the EDZ has passed the interface, the expansion conditions change considerably. The expansion in the substrate material is again comparable to homogeneous bulk materials. In the coating material, the expansion of the EDZ mainly occurs in the sample plane. The transition range between reaching and passing the interface is mainly determined by the "energy conductance" of the interface. A schematic illustration of the situation after passing the interface is shown in Fig. 1 together with the corresponding equations of the energy balance.

## 3. Experimental procedure

The sample material was spin-coated polypropylene (PP) coatings of 6 and 9.8  $\mu\text{m}$  thickness on silicon wafers. The thinner coatings were thermally hardened before investigation. The depth-sensing indentation experiments were performed with a commercially available instrument equipped with a Vickers indenter. The force was increased in steps with a quadratically increasing step height and free selectable waiting periods between the steps. Measurements were performed with end loads of 20, 200 and 1000 mN. The waiting periods between the steps were set between 1 and 10 s.

Prior to the numerical differentiation, five individual measurements were averaged.

## 4. Results

The DLF plots of the investigated samples showed different behaviour for the different end loads. For end loads up to 20 mN and related penetration depths of 1/10–1/7 of the coating thickness, the already reported linear behaviour of  $dF/ds$  versus  $s$  was determined. With increasing penetration depth, however, characteristic deviations from the linear dependence appear. For penetration depths between approximately 1/3 and 2/3 of the coating thickness, a linear dependence between the penetration depth  $s$  and  $(dF/ds)^{1/3}$  or between  $s^3$  and  $dF/ds$  could be proved. An example for these results is shown in Fig. 2. The slope of the linear range was additionally shown to decrease with increasing waiting periods between the force increment steps. A summary of the corresponding results for waiting periods of 1, 5 and 10 s is given in Figs 3 and 4. For identical waiting periods, the two coating systems showed different slopes of the linear ranges in the  $dF/ds$  versus  $s^3$  plots. The slope decrease

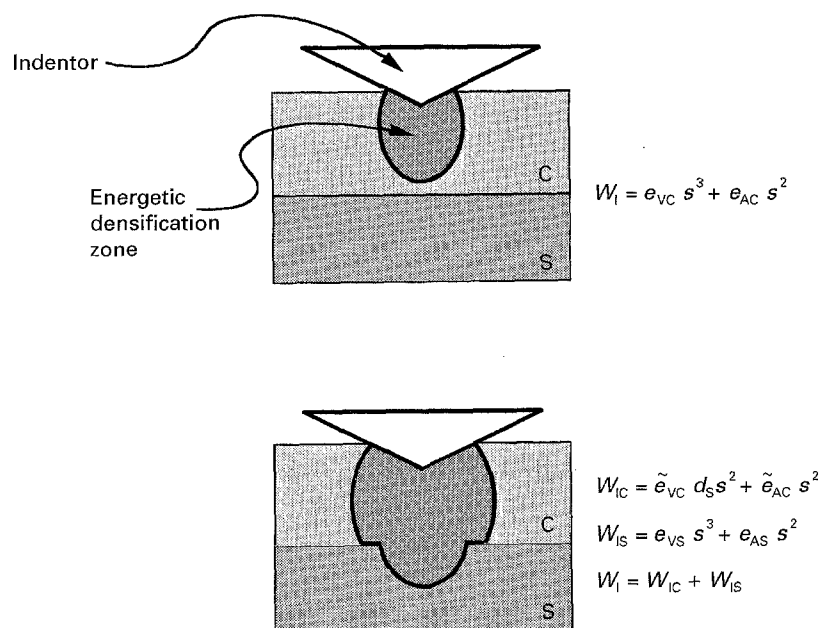


Figure 1 Schematic illustration of the energetic densification zone for coating-substrate systems together with the corresponding energy balance. C, coating; S, substrate.  $W_I$  is the shift energy of the indenter; the additional indices correspond to portions in the coating, C, and substrate, S.  $e_{XY}$ , see comments concerning equations 1 and 3.  $\tilde{e}$ , changed specific energy densities with respect to homogeneous materials.

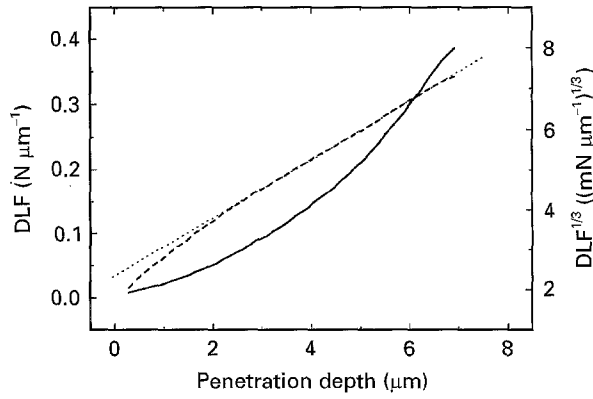


Figure 2 DLF plots for PP coatings on Si, coating thickness 9.8  $\mu\text{m}$ . (—) Primary plot (DLF) and (---) linearized plot (DLF<sup>1/3</sup>). End load = 1000 mN.

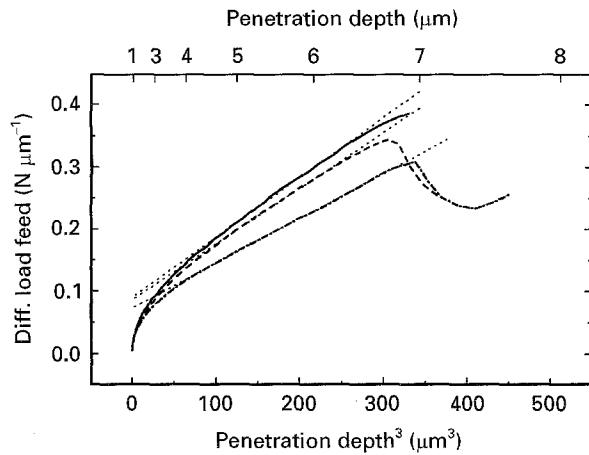


Figure 3 Linearized DLF plot for PP on Si for  $d_c = 9.8 \mu\text{m}$ . (···) Regression lines.  $t_w$  is the waiting period between the load increment steps. (—)  $t_w = 1 \text{ s}$ , slope =  $0.97 \text{ nJ } \mu\text{m}^{-5}$ ; (---)  $t_w = 5 \text{ s}$ , slope =  $0.90 \text{ nJ } \mu\text{m}^{-5}$ ; (-·-)  $t_w = 10 \text{ s}$ , slope =  $0.72 \text{ nJ } \mu\text{m}^{-5}$ .

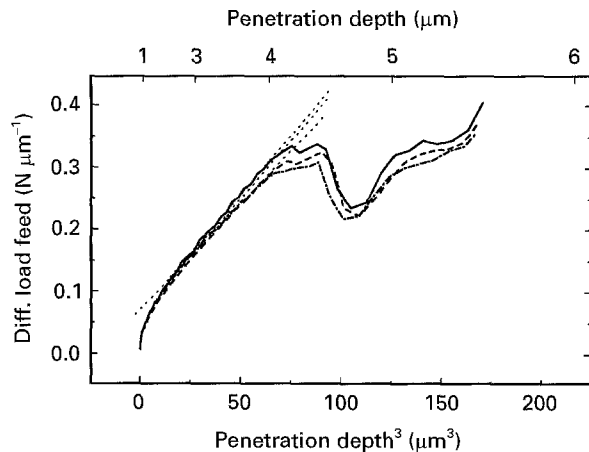


Figure 4 Linearized DLF plot for PP on Si for  $d_c = 6 \mu\text{m}$ . (···) Regression lines.  $t_w$  is the waiting period between the load increment steps. (—)  $t_w = 1 \text{ s}$ , slope =  $3.82 \text{ nJ } \mu\text{m}^{-5}$ ; (---)  $t_w = 5 \text{ s}$ , slope =  $3.62 \text{ nJ } \mu\text{m}^{-5}$ ; (-·-)  $t_w = 10 \text{ s}$ , slope =  $3.43 \text{ nJ } \mu\text{m}^{-5}$ .

versus waiting period proved, however, to be comparable. The corresponding experimental results are illustrated in Fig. 5.

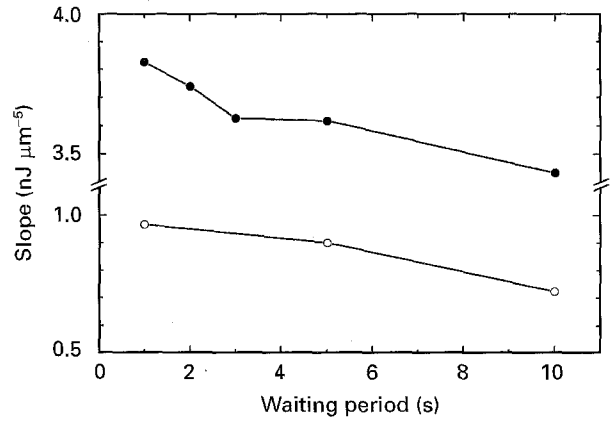


Figure 5 Slope of the linear ranges in the  $dF/ds$  versus  $s$  plots as function of the waiting times between the load increment steps of the indentation experiments. (●) pp, 6  $\mu\text{m}$ ; (○) pp, 9.8  $\mu\text{m}$ .

## 5. Discussion

### 5.1. Modification of the energetic approach

For penetration depths between approximately 1/3 and 2/3 of the coating thickness for all investigated samples, a linear dependence between  $dF/ds$  and  $s^3$  was detected. The energetic approach of Equation 1 has, therefore, to be modified with reference to the viscoelastic and well adhering coatings on hard substrates.

It has already been shown that the mean energy density,  $\bar{w}_V$ , can also be expressed as a product of a mean density,  $n_e$ , of elemental energy carriers with typical energy values,  $w_e$  [8]. With that model the linear behaviour between  $dF/ds$  and  $s^3$  can be described correctly. It is again assumed that the elemental energy carriers are shifted under the action of the penetrating indenter against the resistance of the coating material neighbouring the EDZ. After the outer face of the EDZ reached the interface to the substrate, the resistance into the direction normal to the substrate changes abruptly to infinity. Simultaneously, the viscoelastic properties of the coating material and its good adherence to the substrate limit the motion of the energy carriers parallel to the interface. In front of the contact area between the EDZ and the interface, which is assumed to be circular, an accumulation of energy carriers can be expected. The mean energy density is therefore no longer independent of the penetration depth as it is assumed in Equation 1. In a first approximation, it can be expected to be proportional to  $s^2$ . The energetic approach of Equation 1 thus changes to

$$\begin{aligned} W_I &= n_e k_e s^2 w_e k_V s^3 + \bar{w}_A k_A s^2 \\ &= e_E s^5 + e_A s^2 \end{aligned} \quad (5)$$

with  $k_e$  as a proportionality factor between  $n_e$  and  $s^2$ , as well as  $e_E$  as the indenter-specific density of deformation energy additionally related to the viscoelastic properties of the coating material. In that approach, it is assumed that the shape factors remain independent of the penetration depth. The second derivative of  $W_I$  in relation to  $s$  thus leads to the experimentally determined linear relation between  $dF/ds$  and  $s^3$ . The specific energy,  $e_E$ , follows from the slope of the linear

ranges in the  $dF/ds$  versus  $s^3$  plots. The constancy of  $e_E$  for extended penetration depth ranges suggests its use as a parameter for the mechanical characterization of the coating material investigated here.

### 5.2. Effects of the waiting periods between the force increment steps

The decrease of  $e_E$  with increase of waiting periods between the load steps can also be derived qualitatively by the approach reflected by Equation 5. The viscoelastic properties of the coating and interface permit only a limited motion of the energy carriers parallel to the substrate plane. That motion effects a decrease of the carrier density in the region above the contact range between the EDZ and the substrate. As a consequence, the  $e_E$  value is decreased by increasing waiting periods between the load steps, while the basic relation of Equation 5 is still valid. A reliable quantification of these effects requires, however, extended investigations which could not be performed yet.

### 5.3. Effects of interface strength

The plots of  $dF/ds$  versus  $s^3$  exhibit a maximum after the linear range, followed by a minimum and an adjacent steeper increase closer to the substrate range. The negative slope between the two extremes can be interpreted in analogy to the effects discussed in relation to hard coatings as a release of material stresses parallel to the substrate plane. The effect should, also in analogy to hard coating results, permit calculation of a quantitative measure for compound strength of the PP/Si systems. Again, similar to the effects of the waiting periods, extended investigations are still necessary.

## 6. Conclusion

Depth-sensing indentation measurements were performed on spin-coated polypropylene coatings on sili-

con wafers with a Vickers indenter. The results were correlated to an energy-related evaluation of the deformation processes. As a consequence, the first derivative of the force in relation to the penetration depth is plotted versus the penetration depth to the third power. The approach permits calculation of a constant parameter of the coating material between approximately 1/3 and 2/3 of the coating thickness. That parameter characterizes the resistance of the material to the penetration of the indenter, together with the viscoelastic coating behaviour. Separation and quantification of viscoelastic coating properties, however, require further investigation.

The calculated plots also exhibit effects of the interface at penetration depths in the range of two-thirds of the coating thickness. A quantification of these effects in terms of interface strength, as it was performed for hard coatings, also requires further investigations.

Hence, in summary, the reported results demonstrate the potential of the energy-related interpretation of depth-sensing indentation measurements in connection with polymeric coatings on hard substrates.

## References

1. D. S. SOANE and Z. MARTYENKO, "Polymers in Microelectronics" (Elsevier, Amsterdam 1989).
2. C. R. HEGEDUS, D. F. PULLEY, S. J. SPADADORA, A. T. ENG and D. J. HIRST, *Adv. Mater. Process.* **5** (1989) 62.
3. E. H. LEE, M. P. LEWIS, P. J. BLAU and L. K. MANSUR, *J. Mater. Res.* **6** (1991) 610.
4. E. H. LEE, Y. LEE, W. C. OLIVER and L. K. MANSUR, *ibid.* **8** (1993) 377.
5. B. ROTHER and D. A. DIETRICH, *Phys. Status Solidi (a)* **142** (1994) 389.
6. B. ROTHER, *J. Mater. Sci.* **30** (1995) 5394.
7. B. ROTHER and D. A. DIETRICH, *Thin Solid Films* **250** (1994) 181.
8. B. ROTHER, *Materialwiss. Werkstoff.* **26** (1995) 362.

Received 3 January  
and accepted 8 May 1995